



DeepFake Doctor: Diagnosing and Treating Audio-Video Fake Detection

Marcel Klemt* Carlotta Segna* Anna Rohrbach

TU Darmstadt & Hessian.AI

{marcel.klemt, carlotta.segna, anna.rohrbach}@tu-darmstadt.de

Abstract

Generative AI advances rapidly, allowing the creation of very realistic manipulated video and audio. This progress presents a significant security and ethical threat, as malicious users can exploit DeepFake techniques to spread misinformation. Recent DeepFake detection approaches explore the multimodal (audio-video) threat scenario. In particular, there is a lack of reproducibility and critical issues with existing datasets - such as the recently uncovered silence shortcut in the widely used FakeAVCeleb dataset. Considering the importance of this topic, we aim to gain a deeper understanding of the key issues affecting benchmarking in audio-video DeepFake detection. We examine these challenges through the lens of the three core benchmarking pillars: datasets, detection methods, and evaluation protocols. To address these issues, we spotlight the recent DeepSpeak v1 dataset and are the first to propose an evaluation protocol and benchmark it using SOTA models. We introduce Simple Multimodal BAseline (SIMBA), a competitive yet minimalistic approach that enables the exploration of diverse design choices. We also deepen insights into the issue of audio shortcuts and present a promising mitigation strategy. Finally, we analyze and enhance the evaluation scheme on the widely used FakeAVCeleb dataset. Our findings offer a way forward in the complex area of audio-video DeepFake detection.

1 Introduction

Over the past decade, Generative AI has advanced rapidly, enabling the creation of highly realistic synthetic content. User-friendly applications allow anyone to generate convincing DeepFakes of friends or public figures using just a few seconds of footage. In 2023 alone, over 500,000 fake videos were shared globally [22], reflecting the growing accessibility and impact of this technology. As DeepFakes become more prevalent, so do the risks they pose, namely misinformation and identity manipulation, political interference, and fraud. DeepFakes are now a widespread and serious concern, as they are often used with harmful intent. With continued progress in Generative AI across modalities, including image, video, and audio, there is a rise in multimodal (audio-visual) DeepFakes.

To counter these threats, research on DeepFake detection has grown in parallel with generation techniques. Most of the prior work has explored the unimodal scenarios (predominantly video-only [49, 18, 19], some audio-only [45]). Recent literature is increasingly focused on the multimodal approaches [4, 11, 32, 36, 15] applicable to cases where only one or both modalities are manipulated. As new and increasingly complex approaches are being proposed, dataset issues are being brought to light [5], thus, we may ask: are we in fact making progress in audio-video DeepFake detection?

*Equal contribution

Considering the importance of this topic, *we aim to get a deeper understanding of the key issues prevalent to benchmarking in audio-video DeepFake detection*. We characterize such issues with respect to the three benchmarking pillars: *datasets*, (detection) *methods*, and *evaluation protocols*.

Datasets. In order to train and evaluate multimodal DeepFake detection models, several datasets have been proposed, with the goal to capture both video and audio modality [13, 28, 25, 3, 21, 6, 7, 8, 47, 41, 31]. Yet, most of these datasets suffer from one or more issues. (a) Some of them are not publicly available [8, 47, 41] or have partial availability [21]. (b) Some datasets only offer manipulations for the visual modality, e.g., KoDF [28] and AVLips [31], preventing the study of diverse combinations of manipulated modalities. (c) Datasets like DFDC [13] and AVLips [31] only provide binary labels (real vs. fake) and no manipulation labels, thus not supporting the evaluation of cross-manipulation generalization, which is important for practical applicability. (d) Boldisor *et al.* [5] recently uncovered the presence of *shortcuts* in FakeAVCeleb [25] and AV-DeepFake1M [7] manifested as leading silence which can be exploited by models without having to actually learn the task. (e) Popular datasets, such as FakeAVCeleb, seem to be fairly saturated [36, 18, 19, 17]. Not only is it solved almost to perfection, but it also presents a shortcut. Yet, these datasets form the foundation of this research area. To allow further successful development of multimodal DeepFake detection models and enable measuring the progress, *new open high-quality benchmarks* are required. Besides, we need to deepen our understanding of the *shortcut issue* and find possible mitigation strategies.

Methods. The benchmarking issues are further complicated by often *unavailable DeepFake detection models' implementations*, as many authors do not make their models publicly available [36, 47, 38]. This hinders reproducibility and often makes it impossible to compare to or build upon prior work.

Evaluation Protocols. As already mentioned above, generalization is a crucial aspect when evaluating DeepFake detection methods as they tend to overfit to the training data artifacts and do not generalize beyond [24]. Most prior work includes some form of cross-manipulation (within a dataset) or cross-dataset evaluation. But also here some issues can be found, stemming from mismatched experimental setups used across different works.

Our efforts to address the above issues are as follows. First, we spotlight the dataset previously unexplored for multimodal DeepFake detection, DeepSpeak v1 [3], and make a case for its use as a new benchmark. DeepSpeak v1 contains more recent manipulation techniques, extreme head poses, and occlusions. We also diagnose DeepSpeak v1 regarding the shortcut phenomenon. Additionally, we revisit the popular FakeAVCeleb [25] dataset, where we extend the shortcut analysis offered in [5] to all the manipulations. We provide a manipulation-specific breakdown, showing how all the *fake-audio* manipulations are impacted!

For our benchmarking and analysis, we introduce a new Simple Multimodal Baseline (SIMBA); it features a minimalistic design with two modality encoders (audio&video) followed by a late fusion and a classification head (supported by two unimodal helper heads). Using SIMBA, we study different design choices, such as temporal sampling and augmentation strategies that can be performed at training time. We show that these have a large impact on the model's susceptibility to the shortcuts, offering a *simple and promising mitigation strategy*.

Last, we revise the existing cross-manipulation evaluation protocol on FakeAVCeleb. First, we uncover blind spots (some manipulations were left out!), and manipulation-leakage in the established leave-one-out protocol. We propose new protocols (method and family splits) with different levels of generalization challenges. We are, to the best of our knowledge, the first to present a similar evaluation protocol for DeepSpeak v1 and benchmark SOTA models against it. Lastly, we study cross-dataset generalization with our two benchmarks, spanning the full spectrum of manipulations.

2 Related Work

Multimodal DeepFake Detection Datasets. The DeepFake detection community has introduced various datasets for training and evaluation. These typically feature two video manipulation “families”: *lip synthesis* (lip area only) and *face animation* (entire face). For audio, the most common manipulation is *Text-To-Speech (TTS)*. Datasets are generally categorized into *video-only* and *audio-video* (multimodal) manipulations. Video-only datasets include FaceForensics++ [39], ForgeryNet [20], DF-Platter [33]. Besides AVLips [31], and KoDF [28], contain various video manipulations but only real audio; nonetheless, they are still used in the domain of multimodal DeepFake detection. Audio-video

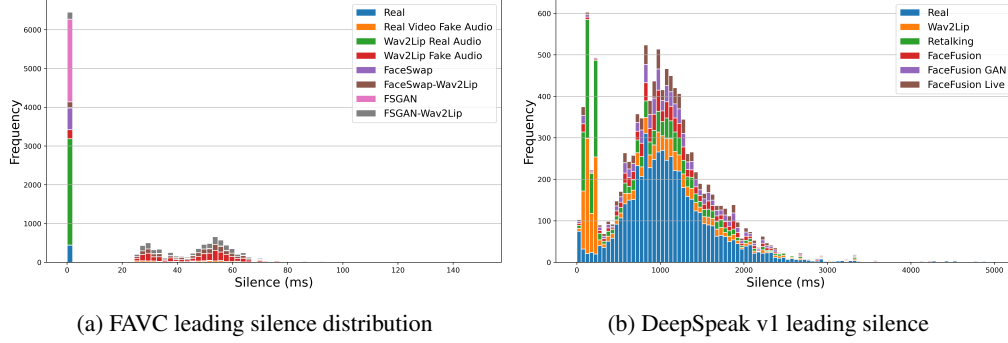


Figure 1: Leading silence distribution of the FAVC and DeepSpeak v1 datasets.

datasets include FakeAVCeleb [25], DeepFake Detection Challenge [13] (DFDC), DeepSpeak v1 [3], Lav-DF [6], PolyGlottFake [21], and AV-DeepFake1M [7]. DFDC uses various manipulations but lacks manipulation-specific labels, thus not supporting cross-manipulation evaluation. Lav-DF and AV-DeepFake1M focus on DeepFake localization (detecting manipulated regions); each uses just one lip synthesis manipulation. FakeAVCeleb and DeepSpeak v1 offer annotated manipulation types, enabling cross-manipulation evaluation. Further, they both include lip synthesis and face animation as generation techniques. PolyGlott introduces multilingual DeepFake scenarios but suffers from missing and low-quality samples.

For our work, we focus on the FakeAVCeleb and DeepSpeak v1 datasets, as they present different labeled types of manipulation in both audio and video modality.

DeepFake Detection Methods. The DeepFake (DF) detection landscape includes both **unimodal** and **multimodal** approaches. Among Unimodal detection approaches, video methods like Lip-Forensics [18] and RealForensics [19] detect artifacts in lips or frames, achieving strong results on FaceForensics++. Audio-based methods transform audio into log spectrograms [44, 46] and use classifiers or capsule networks [45] to capture features and temporal dynamics. Multimodal detection integrates audio and video, typically detecting misalignment between the two modalities [9, 11, 31, 5, 15, 30, 51], phoneme-viseme mismatches [2] or identity shifts [42]. AVoiD-DF [47] uses a Temporal-Spatial Encoder and cross-modal classifier to identify inconsistencies. AVFF [36] reconstructs masked inputs from complementary modalities. Multimodaltrace [38] fuses features via mixer layers and predicts modality labels using a multilabel head.

3 Dataset Analysis

3.1 FakeAVCeleb

Dataset Composition. The dataset FakeAVCeleb [25] is composed of three different video manipulation techniques and one audio manipulation technique. For video, Wav2Lip [37] is used as a lip synthesis technique, whereas FaceSwap [26] and FSGAN [35] are employed for entire face animation. Audio fakes are synthesized using a single method, SV2TTS [23]. Both the lip synthesis and the face animation techniques are either applied alone, generating fakeVideo-realAudio or realVideo-fakeAudio samples, or in combination (fakeVideo-fakeAudio samples). Overall, FakeAVCeleb contains 21k videos from 500 identities, originally selected from the VoxCeleb2 dataset [12]. We provide detailed information about the manipulation distribution in Appendix A.

Shortcut Issue. As recently uncovered, at least part of the FakeAVCeleb dataset suffers from a *leading silence shortcut*. Boldisor *et al.* [5] disclosed that fakeVideo-fakeAudio samples include several milliseconds of silence at the beginning not present in real samples. To further analyze this, we compute the silence by setting a threshold to 20db and consider it only if it lasts at least 20ms. We extend the previous analysis with a manipulation-specific breakdown of leading silences, displayed in Figure 1a. It can be seen that the leading silence is present in all manipulations that involve *fake audio*. As shown by [5], supervised models “latch on” this shortcut to differentiate between real and fake samples, while self-supervised approaches, which do not see fake samples during training, are agnostic to the leading silence. Since FakeAVCeleb is one of the most established datasets in

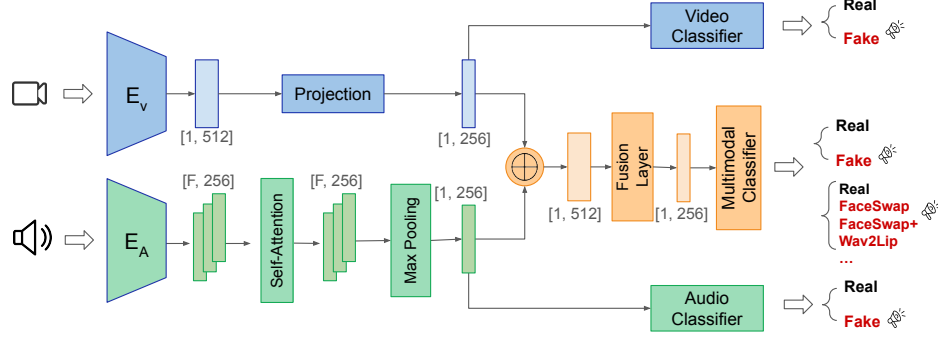


Figure 2: **SIMBA** is composed of two encoders, green for audio and blue for the video. A self-attention and a max pooling layer follow the audio encoder. Each encoder has a modality-specific classifier on top. In the fusion, the embedding vectors are concatenated, \oplus , followed by a fusion layer and a multimodal classifier. We show both the binary and a multiclass variant. (Best viewed in color.)

this research field, this discovery poses the question of whether supervised (especially multimodal) models can still use this dataset and whether the results proposed so far still hold. We discuss our baseline approach in Section 4, where we take the shortcut issue into account.

3.2 DeepSpeak v1

Dataset Composition. The DeepSpeak v1 [3] dataset is composed of five different video and one audio generation technique. Specifically, for video manipulations, it utilizes FaceFusion [40], FaceFusion+GAN [50], FaceFusion Live (FaceFusion but simulating a live streaming environment), Wav2Lip [37] and Video Retalking [10]. ElevenLabs’ voice cloning API [14] is used for generating audio fakes. Unlike FakeAVCeleb, the audio manipulation is only present when a lip synthesis technique is used. The face animation manipulations include solely real audio. Overall, the dataset encompasses 13k videos from 220 identities. More details can be found in Appendix A.

Shortcut Issue. First, we analyze whether leading silence is also present in DeepSpeak v1. The silence is detected by setting the threshold to $20db$ and considering silence only if it lasted at least $20ms$, as for FakeAVCeleb. Figure 1b shows the leading silence histogram over the dataset. Here, the majority of samples have a leading silence of various lengths. Yet, the distribution is balanced between real and fake and along the individual manipulations. The only exception is the first four bins where Wav2Lip and Retalking dominate, raising the possibility of a shortcut.

Both datasets are heavily skewed to the video modality, only featuring a single audio manipulation. Further, they share one manipulation, namely Wav2Lip [37]. We report our findings about the strength of the leading silence shortcut in both datasets in Section 6.3. Further, we include the generalization evaluation for cross-manipulation and cross-dataset in Section 6.4 and 6.5, respectively.

4 Methodology

As previously discussed, one of the challenges we face is the lack of publicly available multimodal detection methods. Many promising models do not release their code or, when it is released, are missing components to make it executable. Thus, we opt to develop SIMBA, our SIMple Multimodal BASeline. SIMBA is a multimodal model, which comprises an audio and video encoder, followed by a fusion branch, trained for the task of DeepFake detection.

Architecture. Figure 2 presents an overview of SIMBA. R(2D+1) [43] is the backbone for our video encoder, initialized from Kinetics pretraining [29]. The idea behind this model is to separate the classical 3D convolution into a 2D+1D convolution. The first one is used to capture spatial features, and the latter one captures temporal features, leading to an efficient and lightweight model originally for the task of action recognition. To reduce the dimensionality of the video encoder output and match it to the audio encoder, a projection layer reduces the video feature from $[1, 512]$ to $[1, 256]$.

Established evaluation protocol							Proposed evaluation protocol							Test set	
	Real Video Fake Audio	Wav2Lip Real Audio	Wav2Lip Fake Audio	FaceSwap Real Audio	FaceSwap + W2L Fake Audio	FSGAN Real Audio	FSGAN + W2L Fake Audio	Real Video Fake Audio	Real Video Real Audio	Wav2Lip Real Audio	Wav2Lip Fake Audio	FaceSwap Real Audio	FaceSwap + W2L Fake Audio	FSGAN Real Audio	FSGAN + W2L Fake Audio
Real Video Fake Audio															
Wav2Lip Real Audio															
Wav2Lip Fake Audio															
FaceSwap															
FSGAN															
				</											

(a) FakeAVCeleb established evaluation protocol. (b) FakeAVCeleb proposed evaluation protocol.

Figure 3: (a) The established vs. (b) our proposed cross-manipulation generalization evaluation for FakeAVCeleb. The top four rows of the proposed evaluation protocol show the different method splits, whereas the last two rows show the family splits Lip Synthesis and Face Animation.

As an audio encoder, we employ the architecture of the BYOL-A model [34], followed by a self-attention layer and max-pooling. The self-attention layer is added to enrich the frame-level features along the temporal dimension. The max-pooling layer removes the noisy features and performs dimensionality reduction from $[F, 256]$, where F is the number of audio frames, to $[1, 256]$.

On top of each unimodal branch, a simple binary classification head is added to distinguish between modality-specific real and fake samples. In this way, the model learns to extract the relevant features for the final multimodal classification task. The outputs of encoders are concatenated to a vector of dimension $[1, 512]$. The final fusion layer reduces the feature dimension to $[1, 256]$, which is given to the final classification head. For the classification, we employ the conventional binary (real/fake) classification, but also investigate a multiclass classification head where each type of manipulation forms its own class (+ the real class). The intuition is that multiclass classification produces a more distinct embedding space during training, which should help generalization. During inference, the multiclass predictions are translated back to a binary prediction score by summing all predicted fake probabilities (i.e., all, except for the real class). This sum serves as a final score to describe the “fakeness” of the corresponding input sample and is comparable to the binary real/fake prediction score. Contrary to the training objective, the evaluation focuses on discovering the presence of a manipulation rather than which specific manipulation it is.

Sampling and Augmentation Strategies. To study the robustness and generalizability of our model, we experiment with several sampling and augmentation strategies during training. Specifically, we study the impact of *temporal jittering* and employ *consecutive frames* vs. *subsampling frames* as our sampling strategies. Temporal jittering describes sampling a clip from the video at a random starting point. This augments the training data and intuitively could increase robustness. N consecutive frames are sampled as the first sampling strategy. For subsampled frames, N frames are sampled with a step size of M . Consecutive frames might provide more information about temporal consistency between two frames, whereas subsampled frames cover a longer temporal window. Concrete hyperparameter choices are provided in Section 6.1.

Loss Functions. Our two model variants, binary and multiclass, leverage two distinct losses. The binary classification head is trained with Binary Cross-Entropy Loss (BCE) [16]. The multiclass classification head is trained with the Cross-Entropy Loss [16] where individual manipulation types serve as class labels (see fig. 2). The unimodal video and audio classifiers are trained using BCE. The final loss is a sum of the unimodal classifiers together with the multimodal classifier, given as $L_{binary} = BCE_{video} + BCE_{audio} + BCE_{multimodal}$ for SIMBA binary and $L_{multiclass} = BCE_{video} + BCE_{audio} + CE_{multimodal}$ for SIMBA multiclass.

5 Evaluation Protocols

Basic Evaluation. The simplest evaluation scheme is to randomly split the data into training and test (e.g., as 70%-30%). In this case, all the manipulations in the test set are also seen in the training set. This scheme typically yields very high performance for supervised approaches, since the models successfully “capture” the specific manipulation artifacts observed during training. However, these optimistic results are not representative of the more realistic case of generalizing to unseen scenarios.

Leave-one-out (Cross-manipulation) Evaluation. As discussed in Section 3, our considered datasets contain multiple video manipulations and a single audio manipulation type. Further, there are “single-

manipulation” and “multi-manipulation” (e.g., using FaceSwap and Wav2Lip in combination) fake samples. The common leave-one-out evaluation, where the model is trained on all the manipulations except the one used for testing, for the FakeAVCeleb dataset (depicted in Fig. 3a) was proposed by [15]. Originally, it was not intended as a leave-one-out evaluation protocol, yet, follow-up works considered it as one [36, 27]. We find several issues with this evaluation protocol. First, some “single-manipulation” samples were completely left out, namely FaceSwap and FS-GAN. Second, the separation of Wav2Lip real audio and Wav2Lip fake audio introduces leakage, presenting no generalization task in the visual modality. Third, some further leakage is introduced with the “multi-manipulation” fakes, e.g., in the Wav2Lip to FS-GAN+Wav2Lip generalization task, as Wav2Lip is used in both the manipulations, but they are considered separately.

To allow a more realistic and challenging cross-manipulation evaluation, we propose method and family splits on FakeAVCeleb (Figure 3b). The cross-manipulation (Figure 3b, top four rows) encompasses one type of video manipulation (“method”) regardless of the audio, e.g., Wav2Lip real and fake audio form one method, whereas FaceSwap and FaceSwap+Wav2Lip form another method. Additionally, we introduce family splits (see Figure 3b, last two rows). The Lip Synthesis Family Split includes every modification that has Wav2Lip (including the combinations with other methods). The Face Animation Family Split consists of all samples that include either FaceSwap or FS-GAN. This results in a stricter, more challenging, and realistic evaluation setting.

Proposed evaluation protocol

	Wav2Lip Real Audio	Wav2Lip Fake Audio	Retalking Real Audio	Retalking Fake Audio	FaceFusion Real Audio	FaceFusion GAN Real Audio	FaceFusion Live Real Audio
Wav2Lip Split							
Retalking Split							
FaceFusion Split							
FaceFusion GAN Split							
FaceFusion Live Split							
Lip Synthesis Family Split							
Face Animation Family Split							

Test set

Figure 4: The proposed evaluation protocol for DeepSpeak v1. The first five rows show method splits, the last two rows are the family splits.

Similarly, we propose the same evaluation concept for DeepSpeak v1, depicted in Figure 4. Again, a method consists of one video manipulation type regardless of the audio. This affects only Wav2Lip and Retalking; Face Fusion, FaceFusion GAN, and FaceFusion Live each form their own split (fig. 4, top 5 rows).

The family split separates the data into the Lip Synthesis vs. Face Animation Family. The Lip Synthesis Family Split includes the Wav2Lip and Retalking method. The Face Animation Family Split encompasses FaceFusion, FaceFusion GAN, and FaceFusion Live (fig. 4, bottom 2 rows). In

this way, we prevent any leakage of similar artifacts between manipulations and present a harder task for cross-manipulation generalization.

Cross-Dataset Evaluation. Another way to evaluate the generalization abilities of models is to train on one dataset and evaluate on another. Generally, this evaluation is carried out by only considering the *shared manipulation type* between the two datasets (no unseen manipulations), as reported by [15, 36]. For example, FakeAVCeleb and KoDF [28] share the Wav2Lip manipulation, thus the evaluation is limited to the Wav2Lip vs. real samples. Hence, the generalization ability of the models is measured in terms of new domains (different lightning, recording setups, etc). We extend cross-dataset evaluation (between FakeAVCeleb and DeepSpeak v1) to cover all manipulations, an ultimate challenge to generalize both in terms of domains and manipulation types.

6 Experimental Results

6.1 Experimental Setup

Data Preprocessing. We preprocess DeepSpeak v1 by cropping and resizing the frames to 224x224 pixels around the face regions utilizing the MTCNN [48] in a similar way as FakeAVCeleb. We set the number of frames to $N = 16$ and a stepsize of $M = 5$ following AVFF [36]. The respective audio is converted to a log-mel spectrogram following [34]. More details are provided in Appendix C.

Metrics. We use average precision (AP) and Area under the curve (AUC). AP is used to measure the precision of the predictions, i.e., the higher the values, the fewer false positives the model predicts. AUC measures how well the model distinguishes between positive and negative classes across all thresholds, where higher is better.

Training Details. We train our SIMBA models with AdamW with $weight_decay = 0.05$ and $eps = 1e - 8$, an initial learning rate of $1e - 4$. A learning rate scheduler reduces the lr after a plateau

of the validation loss for four consecutive epochs. The maximum number of epochs is set to 40, but early stopping intervenes after eight epochs with no validation loss decrease. The batch size is set to 16, distributed among 4xA100 GPUs, and it utilizes ~ 15 GB of space per GPU.

6.2 Benchmarking SIMBA in the basic evaluation

We benchmark our SIMBA model on the standard 70/30% split of the FakeAVCeleb alongside LipForensics [18], RealForensics [19], AVoiD-DF [47], AVAD [15], and AVFF [36]. We show this comparison in Table 1 to assess SIMBA using established protocols, although this has to be treated with caution due to the shortcut found in [5]. SIMBA performs competitively compared to the SOTA unimodal and multimodal models. Thus, we use it alongside other methods in further analysis.

6.3 Analyzing the Leading Silence Shortcut

We use SIMBA as a representative multimodal supervised model to diagnose the silence shortcut in FakeAVCeleb and DeepSpeak v1. At the same time, we investigate the strategies (temporal jittering and consecutive frames vs. subsampling) introduced in Section 4 w.r.t. robustness to the shortcut. Table 2 shows the performance of SIMBA binary and multiclass in a cross-manipulation evaluation on FakeAVCeleb. To see the impact of the shortcut, we evaluate on untrimmed and trimmed videos (that omit the leading silence). AUC values are given on untrimmed videos, and the difference to the trimmed video performance is given in parentheses. SIMBA models with consecutive frames and no temporal jittering latch onto the leading silence shortcut, as shown by a significant negative delta when evaluated on trimmed videos. The same finding holds for SIMBA binary with subsampling, whereas SIMBA multiclass with subsampling seems to be more robust to the shortcut.

Table 1: FakeAVCeleb performance (in %). We use the standard 70/30% split to compare SIMBA to the SOTA multimodal (AVAD, AVFF, AVoiD-DF) and unimodal (Lip-, RealForensics) methods.

Model	Modality	AUC	AP
LipForensics [18]	V	99.81	99.97
RealForensics [19]	V	99.96	100.00
AVoiD-DF [47]	AV	89.20	-
AVAD [15]	AV	79.16	96.09
AVFF [36]	AV	99.10	-
SIMBA binary	AV	99.91	99.99
SIMBA multiclass	AV	99.85	99.98

Introducing the temporal jittering during training reduces the drop in performance between untrimmed and trimmed videos to an almost insignificant delta. Comparing consecutive frames vs. subsampling in models trained with temporal jittering shows that subsampling performs slightly better on average. Specifically, subsampling is most beneficial for the realVideo-fakeAudio split. Notably, *multiclass SIMBAs surpass binary versions on average.*

Table 2: Silence analysis of FakeAVCeleb via a cross-manipulation leave-one-out comparison of multiple SIMBA variants. Performances are given as AUC on untrimmed videos. The difference to the trimmed video performance is given in parentheses. Significant negative differences (> 10) are given in **red**, for a decrease in performance.

	AVG	Wav2Lip Split	realVideo fakeAudio Split	FSGAN Split	FaceSwap Split
Binary consecutive	90.39 (-10.89)	100.00 (-4.08)	74.26 (-35.59)	100.00 (-0.77)	87.30 (-3.11)
Multiclass consecutive	95.24 (-15.76)	99.25 (-9.55)	99.98 (-46.29)	99.98 (-3.69)	81.74 (-3.49)
Binary consecutive jit	87.22 (-0.81)	100.00 (+0.00)	67.09 (-4.14)	99.98 (+0.01)	81.79 (+0.89)
Multiclass consecutive jit	93.91 (-0.17)	99.37 (+0.37)	93.87 (-1.25)	100.00 (+0.00)	82.39 (+0.21)
Binary subsampling	95.15 (-12.51)	100.00 (+0.00)	92.65 (-45.06)	100.00 (-4.03)	87.95 (-0.93)
Multiclass subsampling	94.42 (-1.16)	99.99 (-0.41)	99.98 (-3.60)	100.00 (-0.01)	77.71 (-0.62)
Binary subsampling jit	89.48 (-0.54)	99.98 (+0.00)	81.00 (-1.76)	100.00 (+0.00)	76.93 (-0.40)
Multiclass subsampling jit	95.34 (-0.34)	99.41 (-0.01)	99.32 (-0.86)	100.00 (+0.00)	82.61 (-0.50)

We also diagnose a possible shortcut on DeepSpeak v1 in Table 3, together with the consecutive frames vs. subsampling dimension. Note that both SIMBA models trained on consecutive frames without temporal jittering show a significant negative delta when evaluated on untrimmed vs trimmed

videos. This negative delta is especially present for both models on the Wav2Lip and Retalking split, suggesting that *there is indeed a leading shortcut in these splits*. This supports the observation of the imbalance in the first bins in Figure 1b, where Wav2Lip and Retalking dominate over the other manipulations and Real videos. Besides, SIMBA binary has an unexpected drop on FaceFusion GAN and Live (top row), likely a side-effect of the learned shortcut.

Again, applying temporal jittering to SIMBA models reduces these negative deltas significantly. *This simple and intuitive technique can be easily incorporated in most other multimodal models*. Training with subsampling achieves slightly higher results on average than with consecutive frames, although consecutive frames seem to have a large impact on FaceFusion GAN. Surprisingly, after trimming the silence, the AUC on these samples improves significantly. The difference between SIMBA binary and multiclass is overall not as clear as on FakeAVCeleb.

Table 3: Silence analysis of DeepSpeak v1 via a cross-manipulation leave-one-out comparison of multiple SIMBA variants. Performances are given as AUC on untrimmed videos. The difference to the trimmed video performance is given in parentheses. Significant differences (> 3) are given in red/green for a decrease/increase in performance.

	AVG	Wav2Lip Split	Retalking Split	FaceFusion Split	FaceFusion GAN Split	FaceFusion Live Split
Binary consecutive	91.89 (-5.27)	99.43 (-5.15)	97.42 (-8.23)	92.23 (+0.00)	72.48 (-8.90)	97.87 (-4.08)
Multiclass consecutive	89.97 (-3.00)	98.60 (-4.16)	94.62 (-8.67)	90.31 (-2.93)	68.07 (+0.26)	98.23 (+0.48)
Binary consecutive jit	89.62 (+2.44)	97.86 (+0.38)	87.91 (-2.07)	93.81 (+2.90)	69.63 (+10.03)	98.89 (+0.95)
Multiclass consecutive jit	92.95 (+2.22)	99.39 (+0.20)	91.24 (+2.09)	88.12 (+2.56)	86.06 (+6.20)	99.95 (+0.05)
Binary subsampling jit	93.59 (+0.56)	99.10 (+0.25)	93.80 (+0.36)	96.51 (+0.37)	78.64 (+1.82)	99.89 (+0.01)
Multiclass subsampling jit	93.06 (+0.13)	99.51 (+0.07)	92.44 (-0.26)	95.26 (-0.01)	78.41 (+0.85)	99.70 (+0.00)

6.4 Cross-manipulation Generalization Evaluation

Next, we evaluate models that are robust to the leading silence shortcut using our newly proposed evaluation protocols. Our considered models are Lip-, RealForensics [18, 19], AVAD [15], and our multimodal supervised baseline SIMBA trained with subsampling and temporal jittering (abbr. “jit”). Notice that AVAD is not evaluated in the conventional leave-one-out scenario as it is trained in a self-supervised fashion on LRS2 [1], i.e., it generalizes to all manipulations simultaneously.

Figure 5a shows results using our method splits on FakeAVCeleb. All models show high performance on Wav2Lip, suggesting that *this is the easiest split to generalize to*. The same holds for the FS-GAN split for the supervised models. Hereby, we “reveal” the performance on the FS-GAN realAudio subset, which was hidden in the old evaluation protocol. *The other previously hidden subset is FaceSwap realAudio, which seems to be the hardest subset to generalize to for all models*. Here, the unimodal models achieve higher performance than the multimodal models. We hypothesize that the latter may be slightly more tailored for lip-syncing rather than face animation manipulations.

Results for the method splits on DeepSpeak v1 are shown in Figure 5b. Here, almost all supervised models result in performances $> 90\%$ AUC on the lip synthesis-related splits. All supervised models perform competitively on the different FaceFusion splits. Our method breakdown reveals that FaceFusion GAN split is the hardest to generalize to, whereas FaceFusion Live is the easiest. *The self-supervised AVAD only shows competitive performance when the audio is fake*.

Results for the family splits for both datasets are provided in Appendix E.

6.5 Cross-Dataset Generalization Evaluation

Figure 6 shows performance of Lip-, RealForensics, AVAD, and our SIMBA models in a cross-dataset generalization task, meaning each model was trained on all manipulations of the training dataset and evaluated on all manipulations of the test dataset. Recall that AVAD generalizes from LRS2 to the respective test dataset. As this is a multimodal task, we set the AUCs of the unimodal models to 50% for realVideo-fakeAudio as they can not handle this split.

Surprisingly, *Lip- and RealForensics show very strong generalization performances in both directions*, beating all the other models on average. SIMBA models struggle when generalizing from DeepSpeak v1 to FakeAVCeleb on the realVideo-fakeAudio split, where AVAD’s focus on temporal

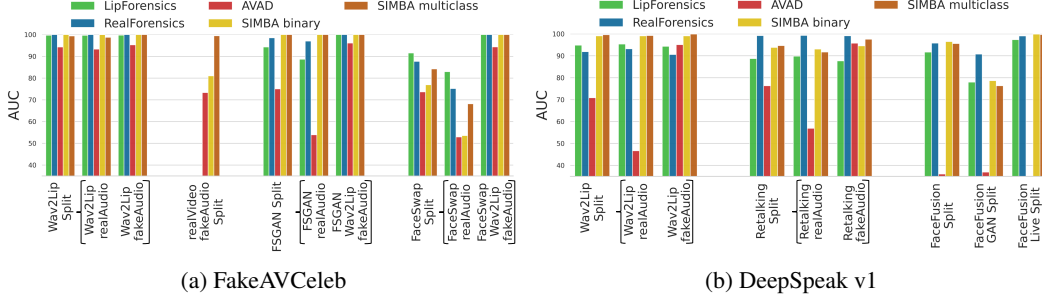


Figure 5: Cross-manipulation comparison using the proposed methods splits (as AUC).

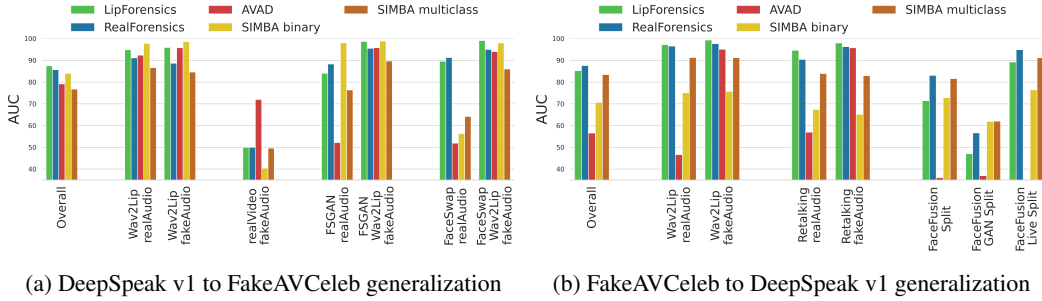


Figure 6: Cross-dataset evaluation across all manipulations (as AUC)

alignment is more beneficial. Interestingly, the results of AVAD on Wav2Lip realAudio are significantly lower on DeepSpeak v1 than on FakeAVCeleb. This hints at a larger domain gap between its training dataset (LRS2) and DeepSpeak v1 compared to the gap between LRS2 and FakeAVCeleb. As DeepSpeak v1 seems to be more out-of-distribution compared to established datasets, it supports our case for using this more recent dataset.

Generalizing from FakeAVCeleb to DeepSpeak v1 is overall a more challenging task, resulting in lower numbers on average. It is interesting that video-only approaches surpass multimodal models on average, despite both datasets including audio manipulations. This underscores that the *datasets are somewhat skewed towards video modality*. Our evaluation shows that *jointly generalizing to a new manipulation and a new dataset is challenging yet not impossible for SOTA methods*.

7 Discussion, Limitations, and Broader Impact

To sum up, in this work, we contributed to the multimodal DeepFake detection by diagnosing the benchmarking issues along the axes of *datasets*, *methods*, and *evaluation protocols*. We showed that the recent DeepSpeak v1 dataset is a suitable benchmark with room for improvement. We presented a baseline method SIMBA, and showed how temporal jittering augmentation scheme leads to robustness to the shortcut issue. We disclosed issues in the existing FakeAVCeleb evaluation protocol, and offered new protocols for both the DeepSpeak v1 and FakeAVCeleb datasets.

Our work has limitations, too, which are partly due to the core issues we aim to address: limited implementation availability of prior approaches makes empirical comparison to these methods challenging. Similarly, various deficiencies of the prior datasets restrict further benchmarking due to the data being unavailable or incompatible with our analysis. We hope that our work overall has a positive societal impact, as we aim to advance the important topic of multimodal DeepFake detection to counter the spread of misinformation. As with any technology, there is some potential for misuse; we can not rule out that our models learn biased representations since the training datasets potentially may contain some biases. We recommend caution when using the models.

Overall, we emphasize the need for new diverse datasets, placing priority on reproducibility and standardized benchmarking, to enable further progress in audio-video DeepFake detection.

Acknowledgement For compute, we gratefully acknowledge support from the hessian.AI Service Center (funded by the Federal Ministry of Education and Research, BMBF, grant no. 01IS22091) and the hessian.AI Innovation Lab (funded by the Hessian Ministry for Digital Strategy and Innovation, grant no. S-DIW04/0013/003).

References

- [1] Triantafyllos Afouras, Joon Son Chung, Andrew W. Senior, Oriol Vinyals, and Andrew Zisserman. Deep audio-visual speech recognition. *IEEE Trans. Pattern Anal. Mach. Intell.*, 44(12): 8717–8727, 2022. doi: 10.1109/TPAMI.2018.2889052. URL <https://doi.org/10.1109/TPAMI.2018.2889052>.
- [2] Shruti Agarwal, Hany Farid, Ohad Fried, and Maneesh Agrawala. Detecting deep-fake videos from phoneme-viseme mismatches. In *2020 IEEE/CVF Conference on Computer Vision and Pattern Recognition, CVPR Workshops 2020, Seattle, WA, USA, June 14-19, 2020*, pages 2814–2822. Computer Vision Foundation / IEEE, 2020. doi: 10.1109/CVPRW50498.2020.00338. URL https://openaccess.thecvf.com/content_CVPRW_2020/html/w39/Agarwal_Detecting_Deep-Fake_Videos_From_Phoneme-Viseme_Mismatches_CVPRW_2020_paper.html.
- [3] Sarah Barrington, Matyas Bohacek, and Hany Farid. Deepspeak dataset v1.0. *CoRR*, abs/2408.05366, 2024. doi: 10.48550/ARXIV.2408.05366. URL <https://doi.org/10.48550/arXiv.2408.05366>.
- [4] Matyas Bohacek and Hany Farid. Lost in translation: Lip-sync deepfake detection from audio-video mismatch. In *Proceedings of the IEEE/CVF Conference on Computer Vision and Pattern Recognition (CVPR) Workshops*, pages 4315–4323, June 2024.
- [5] Dragos-Alexandru Boldisor, Stefan Smeu, Dan Oneata, and Elisabeta Oneata. Circumventing shortcuts in audio-visual deepfake detection datasets with unsupervised learning. *To appear in CVPR*, 2025.
- [6] Zhixi Cai, Kalin Stefanov, Abhinav Dhall, and Munawar Hayat. Do you really mean that? content driven audio-visual deepfake dataset and multimodal method for temporal forgery localization. In *2022 International Conference on Digital Image Computing: Techniques and Applications (DICTA)*, pages 1–10. IEEE, 2022.
- [7] Zhixi Cai, Shreya Ghosh, Aman Pankaj Adatia, Munawar Hayat, Abhinav Dhall, Tom Gedeon, and Kalin Stefanov. Av-deepfake1m: A large-scale llm-driven audio-visual deepfake dataset. In Jianfei Cai, Mohan S. Kankanhalli, Balakrishnan Prabhakaran, Susanne Boll, Ramanathan Subramanian, Liang Zheng, Vivek K. Singh, Pablo César, Lexing Xie, and Dong Xu, editors, *Proceedings of the 32nd ACM International Conference on Multimedia*, pages 7414–7423. ACM, 2024. doi: 10.1145/3664647.3680795. URL <https://doi.org/10.1145/3664647.3680795>.
- [8] Weiling Chen, Sheng Lun Benjamin Chua, Stefan Winkler, and See-Kiong Ng. Trusted media challenge dataset and user study. In Mohammad Al Hasan and Li Xiong, editors, *Proceedings of the 31st ACM International Conference on Information & Knowledge Management, Atlanta, GA, USA, October 17-21, 2022*, pages 3873–3877. ACM, 2022. doi: 10.1145/3511808.3557715. URL <https://doi.org/10.1145/3511808.3557715>.
- [9] Harry Cheng, Yangyang Guo, Tianyi Wang, Qi Li, Xiaojun Chang, and Liqiang Nie. Voice-face homogeneity tells deepfake. *ACM Trans. Multim. Comput. Commun. Appl.*, 20(3):76:1–76:22, 2024. doi: 10.1145/3625231. URL <https://doi.org/10.1145/3625231>.
- [10] Kun Cheng, Xiaodong Cun, Yong Zhang, Menghan Xia, Fei Yin, Mingrui Zhu, Xuan Wang, Jue Wang, and Nannan Wang. Videoretalking: Audio-based lip synchronization for talking head video editing in the wild. In Soon Ki Jung, Jehee Lee, and Adam W. Bargteil, editors, *SIGGRAPH Asia 2022 Conference Papers, SA 2022, Daegu, Republic of Korea, December 6-9, 2022*, pages 30:1–30:9. ACM, 2022. doi: 10.1145/3550469.3555399. URL <https://doi.org/10.1145/3550469.3555399>.

- [11] Komal Chugh, Parul Gupta, Abhinav Dhall, and Ramanathan Subramanian. Not made for each other- audio-visual dissonance-based deepfake detection and localization. In Chang Wen Chen, Rita Cucchiara, Xian-Sheng Hua, Guo-Jun Qi, Elisa Ricci, Zhengyou Zhang, and Roger Zimmermann, editors, *MM '20: The 28th ACM International Conference on Multimedia, Virtual Event / Seattle, WA, USA, October 12-16, 2020*, pages 439–447. ACM, 2020. doi: 10.1145/3394171.3413700. URL <https://doi.org/10.1145/3394171.3413700>.
- [12] J. S. Chung, A. Nagrani, and A. Zisserman. Voxceleb2: Deep speaker recognition. In *INTER-SPEECH*, 2018.
- [13] Brian Dolhansky, Russ Howes, Ben Pflaum, Nicole Baram, and Cristian Canton-Ferrer. The deepfake detection challenge (DFDC) preview dataset. *CoRR*, abs/1910.08854, 2019. URL <http://arxiv.org/abs/1910.08854>.
- [14] ElevenLabs. ElevenLabs: Free Text to Speech & AI Voice Generator. <https://elevenlabs.io/>, 2024. [Accessed 10-11-2024].
- [15] Chao Feng, Ziyang Chen, and Andrew Owens. Self-supervised video forensics by audio-visual anomaly detection. In *Proceedings of the IEEE/CVF Conference on Computer Vision and Pattern Recognition*, pages 10491–10503, 2023.
- [16] I. J. Good. Rational decisions. *Journal of the Royal Statistical Society. Series B (Methodological)*, 14(1):107–114, 1952. ISSN 00359246. URL <http://www.jstor.org/stable/2984087>.
- [17] Zhihao Gu, Yang Chen, Taiping Yao, Shouhong Ding, Jilin Li, Feiyue Huang, and Lizhuang Ma. Spatiotemporal inconsistency learning for deepfake video detection. In Heng Tao Shen, Yueting Zhuang, John R. Smith, Yang Yang, Pablo César, Florian Metze, and Balakrishnan Prabhakaran, editors, *MM '21: ACM Multimedia Conference, Virtual Event, China, October 20 - 24, 2021*, pages 3473–3481. ACM, 2021. doi: 10.1145/3474085.3475508. URL <https://doi.org/10.1145/3474085.3475508>.
- [18] Alexandros Haliassos, Konstantinos Vougioukas, Stavros Petridis, and Maja Pantic. Lips don't lie: A generalisable and robust approach to face forgery detection. In *IEEE Conference on Computer Vision and Pattern Recognition (CVPR)*, pages 5039–5049. Computer Vision Foundation / IEEE, 2021. doi: 10.1109/CVPR46437.2021.00500. URL https://openaccess.thecvf.com/content/CVPR2021/html/Haliassos_Lips_Dont_Lie_A_Generalisable_and_Robust_Approach_To_Face_CVPR_2021_paper.html.
- [19] Alexandros Haliassos, Rodrigo Mira, Stavros Petridis, and Maja Pantic. Leveraging real talking faces via self-supervision for robust forgery detection. In *IEEE/CVF Conference on Computer Vision and Pattern Recognition*, pages 14930–14942. IEEE, 2022. doi: 10.1109/CVPR52688.2022.01453. URL <https://doi.org/10.1109/CVPR52688.2022.01453>.
- [20] Yinan He, Bei Gan, Siyu Chen, Yichun Zhou, Guojun Yin, Luchuan Song, Lu Sheng, Jing Shao, and Ziwei Liu. ForgeryNet: A versatile benchmark for comprehensive forgery analysis. In *IEEE Conference on Computer Vision and Pattern Recognition (CVPR)*, pages 4360–4369. Computer Vision Foundation / IEEE, 2021. doi: 10.1109/CVPR46437.2021.00434. URL https://openaccess.thecvf.com/content/CVPR2021/html/He_ForgeryNet_A_Versatile_Benchmark_for_Comprehensive_Forgery_Analysis_CVPR_2021_paper.html.
- [21] Yang Hou, Haitao Fu, Chuankai Chen, Zida Li, Haoyu Zhang, and Jianjun Zhao. Polyglotfake: A novel multilingual and multimodal deepfake dataset. *CoRR*, abs/2405.08838, 2024. doi: 10.48550/ARXIV.2405.08838. URL <https://doi.org/10.48550/arXiv.2405.08838>.
- [22] Neill Jacobson. Deepfakes and their impact on society, Feb 2024. URL <https://www.openfox.com/deepfakes-and-their-impact-on-society/#:~:text=The%20Growth%20of%20Deepfakes,social%20media%20around%20the%20world>.
- [23] Ye Jia, Yu Zhang, Ron J. Weiss, Quan Wang, Jonathan Shen, Fei Ren, Zhifeng Chen, Patrick Nguyen, Ruoming Pang, Ignacio López-Moreno, and Yonghui Wu. Transfer learning from speaker verification to multispeaker text-to-speech synthesis. In Samy Bengio, Hanna M. Wallach, Hugo Larochelle, Kristen Grauman, Nicolò Cesa-Bianchi, and Roman Garnett, editors, *Advances in Neural Information Processing Systems 31: Annual Conference on Neural*

- Information Processing Systems 2018, NeurIPS 2018, December 3-8, 2018, Montréal, Canada*, pages 4485–4495, 2018. URL <https://proceedings.neurips.cc/paper/2018/hash/6832a7b24bc06775d02b7406880b93fc-Abstract.html>.
- [24] Sarthak Kamat, Shruti Agarwal, Trevor Darrell, and Anna Rohrbach. Revisiting generalizability in deepfake detection: Improving metrics and stabilizing transfer. In *Proceedings of the IEEE/CVF International Conference on Computer Vision*, pages 426–435, 2023.
 - [25] Hasam Khalid, Shahroz Tariq, Minha Kim, and Simon S. Woo. FakeAVCeleb: A novel audio-video multimodal deepfake dataset. In *Thirty-fifth Conference on Neural Information Processing Systems Datasets and Benchmarks Track (Round 2)*, 2021. URL <https://openreview.net/forum?id=TAXFsg6Za0l>.
 - [26] Iryna Korshunova, Wenzhe Shi, Joni Dambre, and Lucas Theis. Fast face-swap using convolutional neural networks. In *IEEE International Conference on Computer Vision, ICCV*, pages 3697–3705. IEEE Computer Society, 2017. doi: 10.1109/ICCV.2017.397. URL <https://doi.org/10.1109/ICCV.2017.397>.
 - [27] Christos Koutlis and Symeon Papadopoulos. Dimodif: Discourse modality-information differentiation for audio-visual deepfake detection and localization. *CoRR*, abs/2411.10193, 2024. doi: 10.48550/ARXIV.2411.10193. URL <https://doi.org/10.48550/arXiv.2411.10193>.
 - [28] Patrick Kwon, Jaeseong You, Gyuhyeon Nam, Sungwoo Park, and Gyeongsu Chae. Kodf: A large-scale korean deepfake detection dataset. In *Proceedings of the IEEE/CVF International Conference on Computer Vision (ICCV)*, pages 10744–10753, October 2021.
 - [29] Ang Li, Meghana Thotakuri, David A. Ross, João Carreira, Alexander Vostroikov, and Andrew Zisserman. The ava-kinetics localized human actions video dataset. *CoRR*, abs/2005.00214, 2020. URL <https://arxiv.org/abs/2005.00214>.
 - [30] Yachao Liang, Min Yu, Gang Li, Jianguo Jiang, Boquan Li, Feng Yu, Ning Zhang, Xiang Meng, and Weiqing Huang. Speechforensics: Audio-visual speech representation learning for face forgery detection. In A. Globerson, L. Mackey, D. Belgrave, A. Fan, U. Paquet, J. Tomczak, and C. Zhang, editors, *Advances in Neural Information Processing Systems*, volume 37, pages 86124–86144. Curran Associates, Inc., 2024. URL https://proceedings.neurips.cc/paper_files/paper/2024/file/9c7900fac04a701cbcd83256b76dbaa3-Paper-Conference.pdf.
 - [31] Weifeng Liu, Tianyi She, Jiawei Liu, Boheng Li, Dongyu Yao, Ziyu Liang, and Run Wang. Lips are lying: Spotting the temporal inconsistency between audio and visual in lip-syncing deepfakes. In A. Globerson, L. Mackey, D. Belgrave, A. Fan, U. Paquet, J. Tomczak, and C. Zhang, editors, *Advances in Neural Information Processing Systems*, volume 37, pages 91131–91155. Curran Associates, Inc., 2024. URL https://proceedings.neurips.cc/paper_files/paper/2024/file/a5a5b0ff87c59172a13342d428b1e033-Paper-Conference.pdf.
 - [32] Trisha Mittal, Uttaran Bhattacharya, Rohan Chandra, Aniket Bera, and Dinesh Manocha. Emotions don’t lie: An audio-visual deepfake detection method using affective cues. In *ACM International Conference on Multimedia*, 2020.
 - [33] Kartik Narayan, Harsh Agarwal, Kartik Thakral, Surbhi Mittal, Mayank Vatsa, and Richa Singh. Df-platter: Multi-face heterogeneous deepfake dataset. In *IEEE/CVF Conference on Computer Vision and Pattern Recognition*, pages 9739–9748. IEEE, 2023. doi: 10.1109/CVPR52729.2023.00939. URL <https://doi.org/10.1109/CVPR52729.2023.00939>.
 - [34] Daisuke Niizumi, Daiki Takeuchi, Yasunori Ohishi, Noboru Harada, and Kunio Kashino. BYOL for audio: Self-supervised learning for general-purpose audio representation. In *International Joint Conference on Neural Networks, IJCNN 2021, Shenzhen, China, July 18-22, 2021*, pages 1–8. IEEE, 2021. doi: 10.1109/IJCNN52387.2021.9534474. URL <https://doi.org/10.1109/IJCNN52387.2021.9534474>.
 - [35] Yuval Nirkin, Yosi Keller, and Tal Hassner. FSGAN: subject agnostic face swapping and reenactment. In *2019 IEEE/CVF International Conference on Computer Vision, ICCV 2019, Seoul, Korea (South), October 27 - November 2, 2019*, pages 7183–7192. IEEE, 2019. doi: 10.1109/ICCV.2019.00728. URL <https://doi.org/10.1109/ICCV.2019.00728>.

- [36] Trevine Oorloff, Surya Koppiseti, Nicolò Bonettini, Divyaraj Solanki, Ben Colman, Yaser Yacoob, Ali Shahriyari, and Gaurav Bharaj. AVFF: audio-visual feature fusion for video deepfake detection. In *IEEE/CVF Conference on Computer Vision and Pattern Recognition, CVPR 2024, Seattle, WA, USA, June 16-22, 2024*, pages 27092–27102. IEEE, 2024. doi: 10.1109/CVPR52733.2024.02559. URL <https://doi.org/10.1109/CVPR52733.2024.02559>.
- [37] K. R. Prajwal, Rudrabha Mukhopadhyay, Vinay P. Namboodiri, and C. V. Jawahar. A lip sync expert is all you need for speech to lip generation in the wild. In Chang Wen Chen, Rita Cucchiara, Xian-Sheng Hua, Guo-Jun Qi, Elisa Ricci, Zhengyou Zhang, and Roger Zimmermann, editors, *MM '20: The 28th ACM International Conference on Multimedia*, pages 484–492. ACM, 2020. doi: 10.1145/3394171.3413532. URL <https://doi.org/10.1145/3394171.3413532>.
- [38] Muhammad Anas Raza and Khalid Mahmood Malik. Multimodaltrace: Deepfake detection using audiovisual representation learning. In *IEEE/CVF Conference on Computer Vision and Pattern Recognition, CVPR 2023 - Workshops, Vancouver, BC, Canada, June 17-24, 2023*, pages 993–1000. IEEE, 2023. doi: 10.1109/CVPRW59228.2023.00106. URL <https://doi.org/10.1109/CVPRW59228.2023.00106>.
- [39] Andreas Rössler, Davide Cozzolino, Luisa Verdoliva, Christian Riess, Justus Thies, and Matthias Nießner. Faceforensics++: Learning to detect manipulated facial images. In *2019 IEEE/CVF International Conference on Computer Vision, ICCV 2019, Seoul, Korea (South), October 27 - November 2, 2019*, pages 1–11. IEEE, 2019. doi: 10.1109/ICCV.2019.00009. URL <https://doi.org/10.1109/ICCV.2019.00009>.
- [40] Henry Ruhs. Facefusion. <https://github.com/facefusion/facefusion>, 2024.
- [41] Asha S, Vinod P, and Varun G. Menon. MMDFD- A multimodal custom dataset for deepfake detection. In *Proceedings of the 2023 Fifteenth International Conference on Contemporary Computing, IC3-2023, Noida, India, August 3-5, 2023*, pages 322–327. ACM, 2023. doi: 10.1145/3607947.3608013. URL <https://doi.org/10.1145/3607947.3608013>.
- [42] Mulin Tian, Mahyar Khayatkhoei, Joe Mathai, and Wael AbdAlmageed. Unsupervised multimodal deepfake detection using intra- and cross-modal inconsistencies. *CoRR*, abs/2311.17088, 2023. doi: 10.48550/ARXIV.2311.17088. URL <https://doi.org/10.48550/arXiv.2311.17088>.
- [43] Du Tran, Heng Wang, Lorenzo Torresani, Jamie Ray, Yann LeCun, and Manohar Paluri. A closer look at spatiotemporal convolutions for action recognition. In *2018 IEEE Conference on Computer Vision and Pattern Recognition, CVPR 2018, Salt Lake City, UT, USA, June 18-22, 2018*, pages 6450–6459. Computer Vision Foundation / IEEE Computer Society, 2018. doi: 10.1109/CVPR.2018.00675. URL http://openaccess.thecvf.com/content_cvpr_2018/html/Tran_A_Closer_Look_CVPR_2018_paper.html.
- [44] Taiba Majid Wani and Irene Amerini. Deepfakes audio detection leveraging audio spectrogram and convolutional neural networks. In Gian Luca Foresti, Andrea Fusiello, and Edwin R. Hancock, editors, *Image Analysis and Processing - ICIAP 2023 - 22nd International Conference, ICIAP 2023, Udine, Italy, September 11-15, 2023, Proceedings, Part II*, volume 14234 of *Lecture Notes in Computer Science*, pages 156–167. Springer, 2023. doi: 10.1007/978-3-031-43153-1_14. URL https://doi.org/10.1007/978-3-031-43153-1_14.
- [45] Taiba Majid Wani, Reeva Gulzar, and Irene Amerini. Abc-capsnet: Attention based cascaded capsule network for audio deepfake detection. In *Proceedings of the IEEE/CVF Conference on Computer Vision and Pattern Recognition (CVPR) Workshops*, pages 2464–2472, June 2024.
- [46] Rui Yan, Cheng Wen, Shuran Zhou, Tingwei Guo, Wei Zou, and Xiangang Li. Audio deepfake detection system with neural stitching for ADD 2022. In *IEEE International Conference on Acoustics, Speech and Signal Processing, ICASSP 2022, Virtual and Singapore, 23-27 May 2022*, pages 9226–9230. IEEE, 2022. doi: 10.1109/ICASSP43922.2022.9746820. URL <https://doi.org/10.1109/ICASSP43922.2022.9746820>.

- [47] Wenyuan Yang, Xiaoyu Zhou, Zhikai Chen, Bofei Guo, Zhongjie Ba, Zhihua Xia, Xiaochun Cao, and Kui Ren. Avoid-df: Audio-visual joint learning for detecting deepfake. *IEEE Trans. Inf. Forensics Secur.*, 18:2015–2029, 2023. doi: 10.1109/TIFS.2023.3262148. URL <https://doi.org/10.1109/TIFS.2023.3262148>.
- [48] Kaipeng Zhang, Zhanpeng Zhang, Zhifeng Li, and Yu Qiao. Joint face detection and alignment using multitask cascaded convolutional networks. *IEEE signal processing letters*, 23(10): 1499–1503, 2016.
- [49] Yinglin Zheng, Jianmin Bao, Dong Chen, Ming Zeng, and Fang Wen. Exploring temporal coherence for more general video face forgery detection. In *Proceedings of the IEEE/CVF International Conference on Computer Vision*, pages 15044–15054, 2021.
- [50] Shangchen Zhou, Kelvin C. K. Chan, Chongyi Li, and Chen Change Loy. Towards robust blind face restoration with codebook lookup transformer. In Sanmi Koyejo, S. Mohamed, A. Agarwal, Danielle Belgrave, K. Cho, and A. Oh, editors, *Advances in Neural Information Processing Systems 35: Annual Conference on Neural Information Processing Systems 2022, NeurIPS 2022, New Orleans, LA, USA, November 28 - December 9, 2022*, 2022. URL http://papers.nips.cc/paper_files/paper/2022/hash/c573258c38d0a3919d8c1364053c45df-Abstract-Conference.html.
- [51] Yipin Zhou and Ser-Nam Lim. Joint audio-visual deepfake detection. In *Proceedings of the IEEE/CVF International Conference on Computer Vision (ICCV)*, pages 14800–14809, October 2021.



DeepFake Doctor: Diagnosing and Treating Audio-Video Fake Detection Supplementary Material

The supplementary materials are organized as follows:

Appendix A presents the details on how the datasets, DeepSpeak v1 and FakeAVCeleb, were split into training, validation, and test sets.

Appendix B provides information on how the metrics of AP and AUC are computed for SIMBA in the multiclass scenario.

Appendix C introduces more details on our experimental setup.

Appendix D validates SIMBA by comparing it to SOTA models on FakeAVCeleb using the established leave-one-out evaluation protocols.

Appendix E shows and discusses the performance of SOTA and SIMBA models using our family splits for FakeAVCeleb and DeepSpeak v1.

Appendix F offers an ablation study on different sampling strategies during inference.

Appendix G offers a graphic representation of the embedding spaces for both the SIMBA binary and multiclass.

A Details on the Datasets

This section introduces some details on how DeepSpeak v1 [3] and FakeAVCeleb [25] are split into training, validation, and test sets, and shows some examples of per-manipulation samples. We introduce a validation set for both datasets, which is used for learning rate scheduling and early stopping. Additionally, the newly introduced set was used for initial architecture decisions and hyperparameter selection. Method and Family Splits are created by leaving out the corresponding manipulations from the training and validation split and then evaluating only these manipulations in the test set. In other words, there is *no leakage* between training plus validation, and test.

DeepSpeak v1 We leave the test set provided by DeepSpeak v1 [3] unchanged, however, we use 20% of the training data as a validation set. Method and Family Splits are constructed in the same way as above: E.g., leaving out FaceFusion in the training and validation set and evaluating on real vs. FaceFusion samples in the test set yields the FaceFusion Split (see fig. 12 for some examples of the samples). In total, the training set encompasses 7,306 samples, the validation set 1,798, and the test set 2,435. Figure 7a provides a detailed breakdown of the number of samples per method split in each set.

FakeAVCeleb We split the FakeAVCeleb [25] into 60% training, 10% validation, and 30% test set based on the identity of the person, obtained from the provided annotations. (For the fakes, we use the source identity of a fake.) Thus, if id-0 is selected as a training identity, the real sample of id-0 and all the fake samples with id-0 as the source identity are included in the training set. Further, the Method Splits are created by removing the corresponding manipulation method from the training and validation set, and evaluating on the respective (held-out) manipulations in the test set. For example, the Wav2Lip Split is created by removing the Wav2Lip method from the training and validation set and evaluating on the real vs. all Wav2Lip samples present in the test set (see fig. 11 for some examples of the samples). The standard split (nothing is held-out) into training, validation, and test set contain 12, 935, 2, 176, and 6, 455 samples, respectively. The resulting number of samples per method split in each set can be found in Figure 7b.

Note that the two datasets are rather different from each other in terms of the amount of real samples: a lot more in the DeepSpeak v1 case, which is a more realistic scenario.

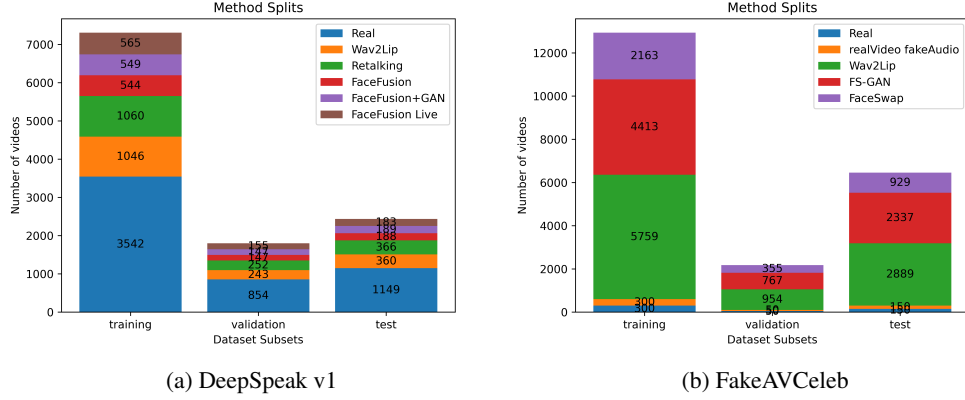


Figure 7: Number of videos for each method split in training, validation, and test for FakeAVCeleb and DeepSpeak v1.

B SIMBA Multiclass Evaluation

SIMBA multiclass predicts a score distribution over all the available training classes. As the final decision we are interested in is a binary decision on whether the test input is real or fake, the multiclass score distribution is post-processed to obtain a single confidence score. For that, all the scores of fake classes from the softmax distribution are summed for each sample:

$$score = \sum_{c=2}^C conf\ score_c, \quad (1)$$

where C is the number of classes and $c = 1$ is the real class. This confidence score is used for AP and AUC calculation. A straightforward approach would be to apply a default threshold of 0.5 for a binary “real”/“fake”-decision, which then can be used to calculate accuracy. However, we found that using the *argmax* operation on the multiclass prediction to determine the most similar (training) class works better. The required binary decision is then obtained by treating every predicted class that is not the real class as fake.

C Detailed Experimental Setup

DeepSpeak Preprocessing We preprocess DeepSpeak v1 [3] by cropping and resizing the frames to 224x224 pixels around the face regions utilizing the MTCNN [48] in a similar way as FakeAVCeleb [25].

Training Details During training, we selected from the video a number of frames equal to $N = 16$ and a stepsize of $M = 5$ following AVFF [36]. Padding is applied where necessary. For audio, we keep the sampling rate of the original audio samples equal to $16000Hz$ for FakeAVCeleb and to $48000Hz$ for DeepSpeak v1. Additionally, the respective audio is converted to a log-mel spectrogram, with a $n_{fft} = 321$ and $n_{mels} = 64$, following BYOL-A settings [34]. The audio is then normalized by computing the *log* of the spectrogram and normalizing this value with the mean and standard deviation, computed among the audio samples of the dataset.

Regarding the hyperparameters, the learning rate is $1e - 4$ and we use the *ReduceLROnPlateau*, with a patience of 4 epochs. The total number of epochs is 40, with an Early Stopping value of 8 epochs.

The self-attention layer after the audio encoder is defined with a number of layers equal to 2 and of attention heads equal to 8.

D Validating SIMBA

Besides validating our SIMBA models on the 70/30 split (Tab. 1), we benchmark SIMBA using the former “leave-one-out” evaluation schema (Fig. 3a) on FakeAVCeleb in Table 4. SIMBA results are

comparable, or even better, than current SOTA models. Especially strong is SIMBA on the rV-fA split where it reaches almost 99% AUC, surpassing the other two multimodal models and underlining the strengths of SIMBA’s audio encoder. This supports our use of SIMBA as a supervised multimodal analysis tool.

Table 4: Leave-one-out comparison between SIMBA and SOTA. We consider the established leave-one-out protocol on FakeAVCeleb. Performance in %. Abbreviations: rV – real Video, rA – real Audio, fA – fake Audio, W2L – Wav2Lip.

Model	Modality	rV+fA		W2L+rA		faceswap+fA		fsgan+fA		W2L+fA	
		AP	AUC	AP	AUC	AP	AUC	AP	AUC	AP	AUC
LipForensics [18]	V	-	-	100.00	100.00	99.98	99.94	100.00	99.99	99.95	99.84
RealForensics [19]	V	-	-	99.97	99.87	99.98	99.91	99.99	99.94	99.70	99.21
AVAD [15]	AV	62.40	71.60	93.60	93.70	95.30	95.80	94.10	94.30	93.80	94.10
AVFF [36]	AV	93.30	92.40	94.80	98.20	100.00	100.00	99.90	100.00	99.40	99.80
SIMBA binary	AV	99.79	98.76	91.20	95.63	100.00	100.00	100.00	100.00	100.00	100.00
SIMBA multiclass	AV	99.84	98.91	94.71	96.88	100.00	100.00	100.00	100.00	100.00	100.00

E Family Split Performance

Figure 8 shows the performance of SOTA models [18, 19, 15] and SIMBA models trained with subsampling and temporal jittering on our family splits introduced in Section 5. Generalizing to the Lip Synthesis Family split results in overall high performance on FakeAVCeleb. Especially SIMBA generalizes perfectly. AVAD achieves slightly higher performance when the audio is fake, suggesting that it slightly over-relies on the auditory modality. The unimodal models generalize perfectly when they face a face animation manipulation together with Wav2Lip but reach slightly lower results on only Wav2Lip. *The combination of multiple manipulations seems to amplify the “fake” signal from which the models benefit.* This finding is also confirmed on the Face Animation Family Split, which shows perfect scores for the supervised models on FS-GAN/FaceSwap + Wav2Lip. AVAD struggles with real audio, which was already found in the method split (Sec. 6.4). We can also confirm from the method split that FaceSwap is the hardest split for all models. Even though it has artifacts easily detectable by humans, it seems these artifacts are not shared with any other manipulation, making it much harder to generalize to. Overall, the performance is lower on the Face Animation Family than the Lip Synthesis Family Split, revealing that *it is more challenging to generalize from lip synthesis manipulation to face animation manipulations than vice versa.*

Family Split results on DeepSpeak v1 are visualized in Figure 8b. Scores drop significantly on the Lip Synthesis Family Split on DeepSpeak v1 compared to FakeAVCeleb. This suggests that FaceSwap and FS-GAN have more in common with Wav2Lip than the more recent FaceFusion manipulations. AVAD’s alignment focus helps detect fake audio splits, as it surpasses all other models on these. SIMBA models outperform the unimodal models on the Lip Synthesis Split even though it was trained only on real audio, thus, has no benefit out of its multimodality. Already the visual branch of SIMBA provides generalization capabilities. On the face animation family split, SIMBA is outperformed by RealForensics. This split is purely real audio, and it seems the fake audio during training hurts SIMBA’s generalization capabilities. FaceFusion GAN is the hardest split to generalize to, whereas FaceFusion Live is the easiest, which is the same finding as for the method split (Sec. 6.4). On average, performance is much lower on DeepSpeak v1 and on FakeAVCeleb, showing that *the more recent manipulations of DeepSpeak v1 present a harder generalization challenge for SOTA models.*

Finally, the family split performance is lower than the method split results, highlighting that *the more realistic family splits actually pose a greater generalization challenge for SOTA models.*

F Ablation of the Sampling Strategy During Evaluation

As different SOTA models use different sampling strategies when evaluating, we investigate three different sampling strategies for SIMBA in Table 5. First, we sample one clip starting from the beginning. Second, multiple clips are sampled from the video, and the prediction scores are aggregated via the mean operation (*clips mean*). Last, multiple clips are sampled and aggregated with the max operation (*clips max*). Each clip is 80 frames long (subsampling stepsize * number of frames:

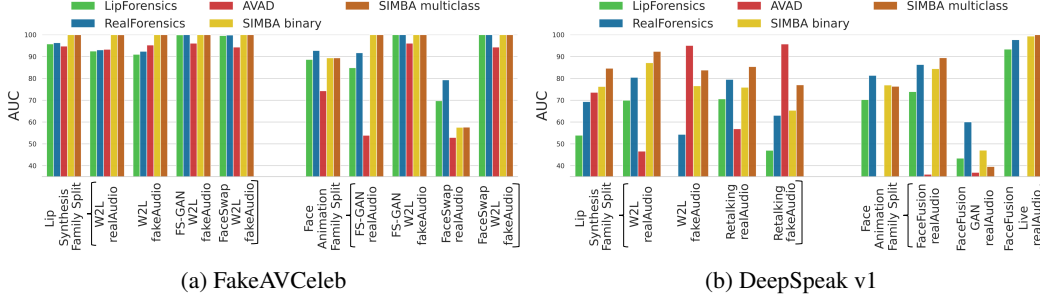


Figure 8: Cross-manipulation comparison using the proposed family splits (as AUC).

$5 * 16 = 80$). When multiple clips are sampled per video, as many clips are sampled with no overlap as can be extracted from the entire video. Yet, the maximum number of clips per video is set to five. We found out that aggregating multiple clips hurts the generalization performance. Consequently, we report results with the *beginning* schema in the paper.

Table 5: Evaluation sampling strategy analysis of DeepSpeak v1 via a cross-manipulation leave-one-out comparison of SIMBA binary and multiclass trained with subsampling and temporal jittering. Performance is given as AUC.

	AVG	Wav2Lip Split	Retalking Split	FaceFusion Split	FaceFusion GAN Split	FaceFusion Live Split
Binary beginning	93.59	99.10	93.80	96.51	78.64	99.89
Binary clips mean	91.02	99.15	92.27	94.30	69.54	99.83
Binary clips max	90.47	98.81	90.60	93.85	69.23	99.86
Multiclass beginning	93.06	99.51	92.44	95.26	78.41	99.70
Multiclass clips mean	90.78	98.98	89.10	92.61	73.60	99.63
Multiclass clips max	91.28	99.03	90.15	92.99	74.56	99.66

G Visualizing SIMBA’s Embedding Spaces

Figure 9 visualizes the embedding space of SIMBA binary and SIMBA multiclass on the FS-GAN and FaceSwap method split of FakeAVCeleb using t-distributed stochastic neighbor embedding (t-SNE)². The figure plots the in-distribution manipulations (seen during training) as \circ and the out-of-distribution samples (unseen manipulations) as \times .

Notice that the multiclass models form clear, distinct clusters for each in-distribution manipulation type (Fig. 9c, 9d). In contrast to that, Wav2Lip fake audio overlaps with FaceSwap+Wav2Lip and Wav2Lip real audio overlaps with FaceSwap for SIMBA binary on the FS-GAN split (Fig. 9a). Similarly, Wav2Lip fake audio overlaps with FS-GAN+Wav2Lip and Wav2Lip real audio overlaps with FS-GAN for SIMBA binary on the FaceSwap split (Fig. 9b). Notice that these overlaps are audio-related. *The binary models form real-video-real-audio, real-video-fake-audio, fake-video-real-audio, and fake-video-fake-audio clusters.*

Unseen manipulations during training are aligned to existing clusters during inference. The SIMBA binary model on the FS-GAN split maps nicely the FS-GAN samples to the Wav2Lip real audio / FaceSwap cluster, the FS-GAN+Wav2Lip samples to the Wav2Lip fake audio / FaceSwap+Wav2Lip cluster, and the real samples to the real cluster. The corresponding multiclass model (Fig. 9c maps the FaceSwap+Wav2Lip samples to Wav2Lip fake audio and to the FaceSwap+Wav2Lip cluster and the real samples to the real cluster. Yet, the FS-GAN samples are aligned with the Wav2Lip real audio cluster and not with the FaceSwap cluster. This reveals that *for SIMBA, FS-GAN has more learned artifacts in common with the lip synthesis manipulation Wav2Lip than with the face animation*

²Geoffrey E. Hinton, and Sam Roweis. Stochastic neighbor embedding. In *Advances in neural information processing systems*, 15, 2002.

manipulation FaceSwap. Still, no manipulation overlaps with the real cluster, resulting in the almost perfect generalization performance of SIMBA in Figure 5a.

The FaceSwap real audio manipulation is the hardest manipulation to generalize to for SIMBA (Fig. 5a). The embedding spaces of SIMBA on the FaceSwap split show a high overlap between the FaceSwap real audio and real cluster. The FaceSwap+Wav2Lip fake audio is perfectly aligned with the fake-video-fake-audio cluster (Fig. 9b). The multiclass SIMBA aligns the unseen FaceSwap+Wav2Lip with the Wav2Lip fake audio and not with the FS-GAN+Wav2Lip cluster. This shows that *the Wav2Lip part of the combined manipulation has a greater impact on the final decision than the face animation part for SIMBA*. SIMBA's performance drops when generalizing to the FaceSwap real audio manipulation compared to the FS-GAN real audio manipulation can be explained by the multiclass embedding spaces. *Since FS-GAN and FaceSwap do not share artifacts (for SIMBA), and only FS-GAN shares artifacts with Wav2Lip, the unseen FaceSwap real audio manipulation is not aligned with any seen manipulation but with the real cluster.*

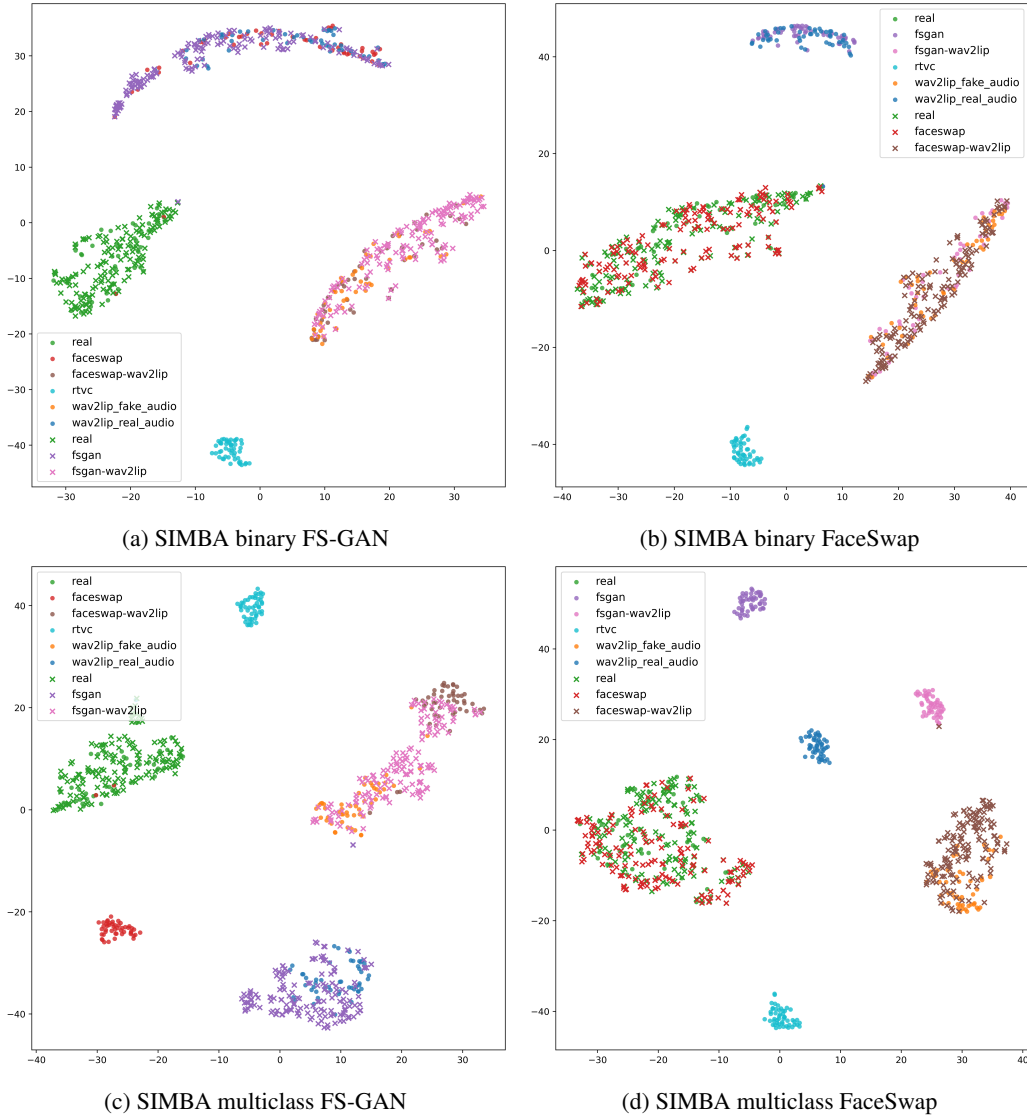


Figure 9: Visualization of the embedding space for SIMBA binary and multiclass on FakeAVCeleb. The left column shows SIMBA models trained on the FS-GAN method split, whereas the FaceSwap method split was used for the right column. \circ show manipulations seen during training and \times the unseen manipulations.

Figure 10 displays the embedding spaces of SIMBA binary and SIMBA multiclass on the Wav2Lip and Retalking method split of DeepSpeak v1. As DeepSpeak v1 does not have a real-video-fake-audio combination, the binary models form roughly three clusters (real-video-real-audio, fake-video-real-audio, and fake-video-fake-audio). SIMBA binary on the Wav2Lip split aligns Wav2Lip real audio with the fake-video-real-audio cluster and Wav2Lip fake audio with the fake-audio cluster, resulting in almost perfect generalization performance as discussed in Section 6.4. The same holds for SIMBA multiclass on the Wav2Lip split (Fig. 10c). Yet, Wav2Lip fake audio forms a new cluster close to the Retalking clusters, and Wav2Lip real audio samples are aligned with the FaceFusion Live cluster, suggesting that *the Wav2Lip real audio lip synthesis manipulation has more in common with the face animation manipulation FaceFusion Live than with the Retalking lip manipulation.*

When generalizing to the Retalking split, SIMBA’s performance is slightly lower than on the Wav2Lip split (Fig. 5b). This is caused by the slight overlap between the Retalking real audio samples and the real cluster for SIMBA binary as well as multiclass. Comparing the embedding spaces from FakeAVCeleb to the ones on DeepSpeak v1 reveals that some unseen DeepSpeak v1-manipulations form clusters which do not match existing clusters. Unseen FakeAVCeleb-samples always show a high overlap with existing clusters. This suggests that *the more recent manipulation techniques generate more dissimilar artifacts than the older manipulation techniques present in FakeAVCeleb.*

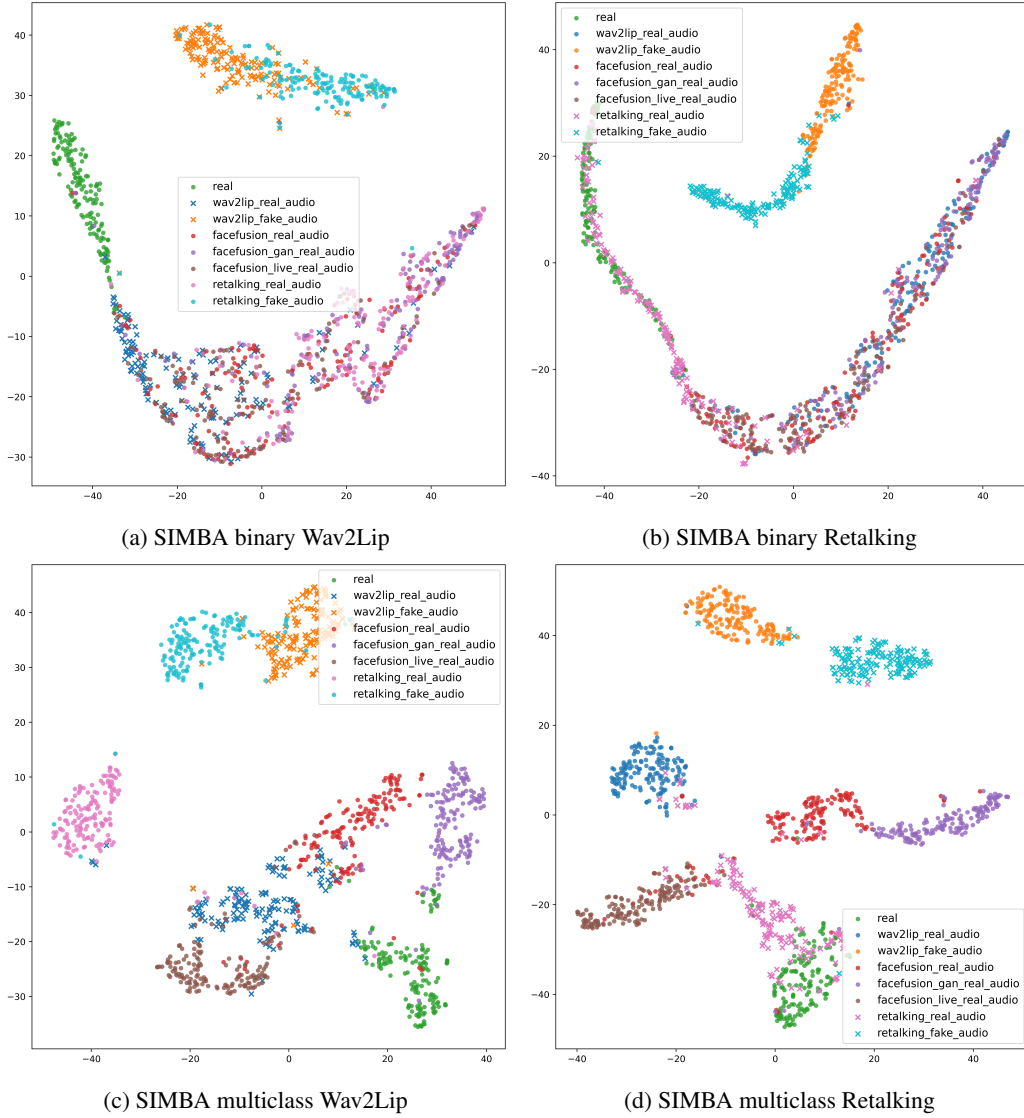


Figure 10: Visualization of the embedding space for SIMBA binary and multiclass on DeepSpeak v1. The left column shows SIMBA models trained on the Wav2Lip method split, whereas the Retalking method split was used for the right column. \circ show manipulations seen during training and \times the unseen manipulations.

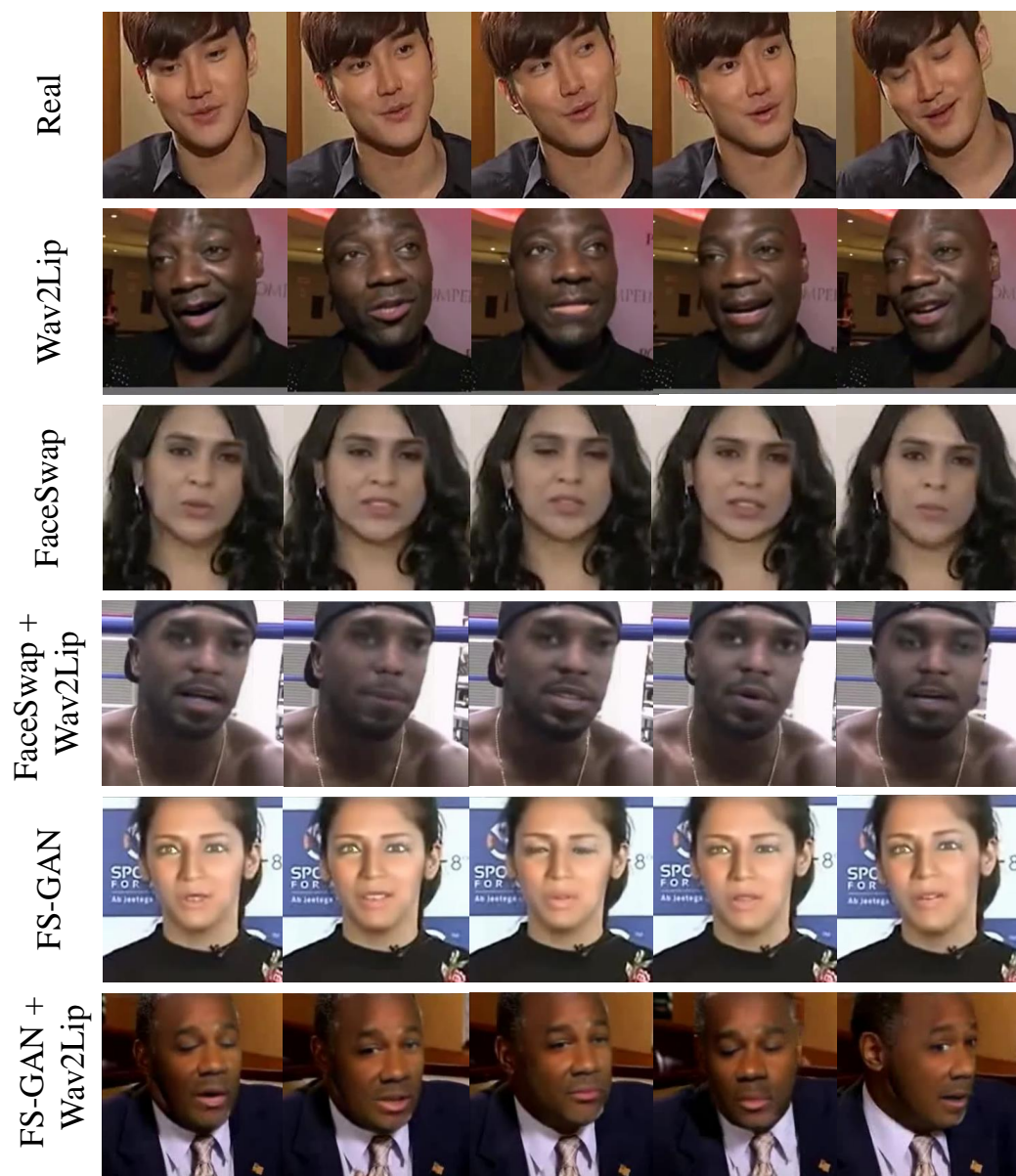


Figure 11: Examples of the video manipulation types in FakeAVCeleb.

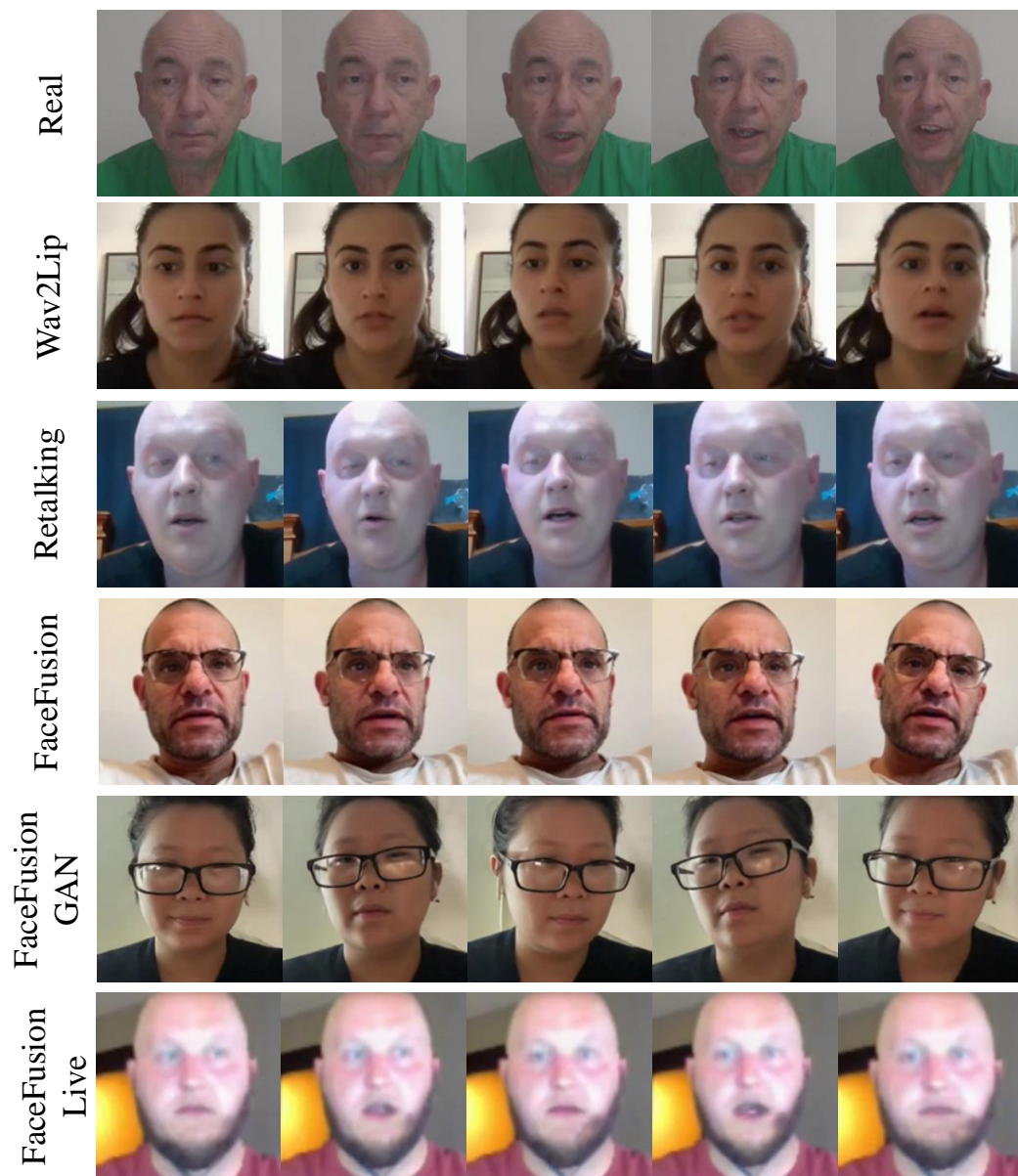


Figure 12: Examples of the video manipulation types in DeepSpeak v1.